Finite Element Investigation of Stentless Pericardial Aortic Valves: Relevance of Leaflet Geometry

Fang Li Xiong,[1] Wolfgang A. Goetz,[2] Chuh Khiun Chong,[3] Yeow Leng Chua,[4] Stefan Pfeifer,[5] Erich Wintermantel,[5] and Joon Hock Yeo[1]

[1]School of Mechanical and Aerospace Engineering, Nanyang Technological University, 50 Nanyang Avenue, Singapore 639798, Singapore; [2]Clinic for Cardiovascular Surgery, German Heart Center Technical University Munich, Munich, Germany; [3]Department of Engineering Materials, University of Sheffield, Sheffield, UK; [4]Department of Cardiothoracic Surgery, National Heart Center, Singapore, Singapore; and [5]Department for Medical Engineering, Technical University Munich, Garching, Germany

Abstract—Recent developments in aortic valve replacement include the truly stentless pericardial bioprostheses with single point attached commissures (SPAC) implantation technique. The leaflet geometry available for the SPAC valves can either be a simple tubular or a complex three-dimensional structure molded using specially designed molds. Our main objective was to compare these two leaflet designs, the tubular vs. the molded, by dynamic finite element simulation. Time-varying physiological pressure loadings over a full cardiac cycle were simulated using ABAQUS. Dynamic leaflet behavior, leaflet coaptation parameters, and stress distribution were compared. The maximum effective valve orifice area during systole is 633.5 mm^2 in the molded valve vs. 400.6 mm^2 in the tubular valve, and the leaflet coaptation height during diastole is 4.5 mm in the former, in contrast to 1.6 mm in the latter. Computed compressive stress indicates high magnitudes at the commissures and inter-leaflet margins of the tubular valve, the highest being 3.83 MPa, more than twice greater than 1.80 MPa in the molded valve. The molded leaflet design which resembles the native valve exerts a positive influence on the mechanical performance of the SPAC pericardial valves compared with the simple tubular design. This may suggest enhanced valve efficacy and durability.

Keywords—Single point attached commissures, Valve molds, Dynamic leaflet behavior, Effective valve orifice area, Coaptation height, Coaptation area, Compressive stress.

INTRODUCTION

Bioprosthetic aortic valves, with the benefit of avoiding anticoagulation, have been implanted extensively. A stent and sewing ring are often used in bioprosthetic valves to provide support to the leaflets and to facilitate implantation with a short ischemic time, but these clearly obstruct the flow, inducing steep transvalvular pressure gradients and high stress on the leaflets, two characteristics that translate into early structural valve deterioration.[28,33] Various stentless xenografts have been developed to improve outcomes, though most of them still have inherent obstructive features as they require support with a Dacron cloth and original aortic root.[1,26] The truly stentless solution has generally been hampered by the complexity of the implantation and the high technical demand on the operating surgeon.[26] Of tremendous interest is to design a bioprosthetic aortic valve that is not only truly stentless, but also simple and fast to implant.

Recent developments of aortic valves with full pericardial constructs, aided by the single point attached commissures (SPAC) implantation technique, offer this possibility.[8,14,15,25] These SPAC pericardial valves are implanted with the base of the valve sutured to the aortic root in a circular line and the commissures to the aortic wall at the level of sinotubular junction at only three single points, which greatly simplifies the implantation procedure. The SPAC technique has proved its efficiency and reliability in clinical settings.[12,16]

Leaflet geometry is believed to be important for the efficacy and longevity of bioprosthetic aortic valves. Currently, two leaflet geometric designs can be identified for the SPAC stentless pericardial valves: a simple tubular geometry and a complex three-dimensional (3D) structure molded using specially designed valve molds.[8,12,14–16,25] The main objective of this study was to elucidate the influence of the two leaflet geometric

designs, the tubular and the molded, on the mechanical performance of the SPAC pericardial valves. We hypothesized that the molded 3D leaflet geometry which resembles the native aortic valve would perform better than the simple tubular leaflet geometry. We also compared the SPAC molded valve model with a conventional valve model to examine if the SPAC approach would in any way compromise the valve performance. The two models are similar in leaflet geometry, but the conventional model uses the conventional implantation approach with sutures placed all along the scalloped leaflet attachment line. Critical valve performance parameters including leaflet deformation, effective valve orifice area (EVOA), coaptation parameters, and stress distribution on the leaflets were analyzed. A dynamic finite element analysis was used to calculate these parameters with sufficient data resolution and to capture leaflet dynamics in microseconds. It is hoped that this study would yield a better understanding of the relevance of leaflet geometry to the functioning of the SPAC valves.

METHODS

Model Geometry

The aortic root was modeled as a circular conduit of internal diameter 25 mm, characterized by the three protruding sinuses of symmetrical hemispheres. Three surface models representing, respectively, a SPAC tubular valve, a SPAC molded valve, and a conventional valve incorporating the aortic root were created. Figure 1 illustrates the differences in the implantation

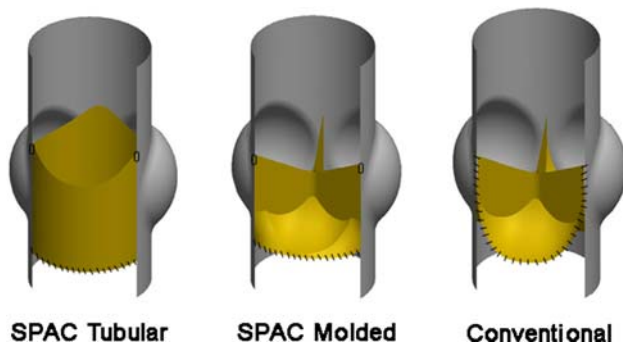SPAC Tubular   SPAC Molded   Conventional

FIGURE 1. Schematic representation of the SPAC tubular, SPAC molded, and conventional valve models, illustrating differences in implantation approach and leaflet geometry. One-third of the aortic root is removed for visualization of the internal structure. For the SPAC implantation approach, the base of the valve is sutured to the aortic annulus in a circular line and the commissures attached to the aortic wall at the level of sinotubular junction at three single points, while for the conventional approach, running sutures are placed following the scalloped leaflet attachment line. The small rectangular tabs represent three commissural attachment points.

approach and the leaflet geometric design between the three models. The tubular valve, which is evolved from a simple cylindrical tube, has a leaflet geometry following the surface of one-third of a cylinder with its free edges slightly scalloped, corresponding to a fully opened valve configuration.[8] The leaflet of the conventional valve is designed, using the design parameters reported by Thubrikar[31] for the optimization of leaflet geometry, to represent the configuration of a closed valve. For the SPAC molded valve, the leaflet geometry is similar to that of the conventional valve; the leaflet height, the free edge length, and the 3D leaflet profile are identical, but the leaflet area is extended to fill up the inter-leaflet triangles to allow for the application of the SPAC technique. The important dimensions for each model are displayed in Table 1.

The surface models were meshed using 4-node, doubly curved quadrilateral shell elements with reduced integration. Enhanced hourglass control was applied to avoid excessive distortion of the elements and to control the mode of zero energy. The aortic root shell model consists of 4446 elements with a uniform thickness of 1.5 mm, while the valve models consist of 4662–5460 elements, depending on the differences in valve geometry, with a uniform thickness of 0.4 mm. The Simpson's rule with five integration points through the shell thickness was specified to calculate the cross-sectional behavior of the shell model.

Properties of Material

All model materials were assumed to be isotropic and homogenous. Although the fresh pericardial tissue is an anisotropic material, there is evidence that the pericardial tissue after the fixation process acts more like a homogeneous isotropic material.[18,21] An elastic modulus of 8 MPa and a density of 1100 kg m^{-3} were assigned to the pericardial leaflet tissue; these values are within the statistical range of the treated pericardial tissue.[34] The aortic root wall was modeled to be flexible, with a modulus and density of 2 MPa and 2000 kg m^{-3}, respectively. The poisson ratio was set at 0.45 for all tissue materials to account for the near-incompressible behavior of the soft tissue.

Loadings and Solution Procedure

All three models were assumed to be stress-free in the naturally opened valve configuration. Boundary conditions were assigned to the aortic root model such that its top and bottom boundaries were constrained in the up-and-down direction, but radial expansion was allowed. The valves were connected to the aortic root wall by specifying tie constraints. For the SPAC tubular and the molded valve models, the base was tied

TABLE 1. Design parameters of the models and summary of important results.

	SPAC tubular	SPAC molded	Conventional
Design parameters			
d_b/d_c (mm)	25/25	25/25	25/25
H (mm)	25	21.6	21.6
H_s (mm)	2	2	4
L (mm)	20	21.9	21.9
L_f (mm)	28.2	29.2	29.2
A (mm^2)	563.6	619.5	561.3
Summary of results			
EVOA (mm^2)	400.6	630.8	633.5
C_c (mm)	1.2	4.5	4.4
A_c (%)	41.5	61.3	51.7
Max compressive stress magnitude (MPa)	3.83	1.80	2.13
Max Von Mises stress (MPa)	3.40	3.67	3.92

d_b, Diameter of valve at the base; d_c, diameter of valve at the commissures; H, overall valve height from the bottom of the valve base to the top of the commissures; H_s, commissural attachment length or commissural height; L, leaflet length in radial direction; L_f, free-edge length; A, leaflet surface area; EVOA, effective valve orifice area at fully opened position; C_c, maximum coaptation height; A_c, percentage of maximum coaptation area to leaflet surface area.

at the position just below the sinuses and the three commissures were tied to the sinotubular junction by a 2-mm vertical line. For the conventional valve model, tie constraints were specified along the entire scalloped leaflet edge. Three kinematic contacts were defined to simulate interactions and to prevent penetration between the surfaces: contact between the aortic inner surface and the valve outer surface, self-contact of the valve inner surface, and self-contact of the valve outer surface.

For application of loadings, the aortic root model was divided into the upper (aortic) and the lower (ventricular) walls at the level where the valve bottom edge was tied. Prior to dynamic simulation, diastolic pressures of 81.9, 10.3, and 71.6 mmHg, which correspond to the initial values of the three pressure waveforms (at $t = 0$ s in Fig. 2), were gradually applied on the aortic wall, ventricular wall and valve leaflets, respectively. Starting from this closed, diastolic, stressed configuration, time-varying and spatially uniform physiological pressure loadings over a full cardiac cycle of 0.9 s (Fig. 2) were applied in each of these cases: the aortic pressure waveform on the aortic wall, the left ventricular pressure waveform on the ventricular wall, and the aorto-ventricular pressure gradient on the valve leaflets. The fully nonlinear finite element code ABAQUS 6.7 (ABAQUS, Inc., Pawtucket, RI) was used for all analysis runs.
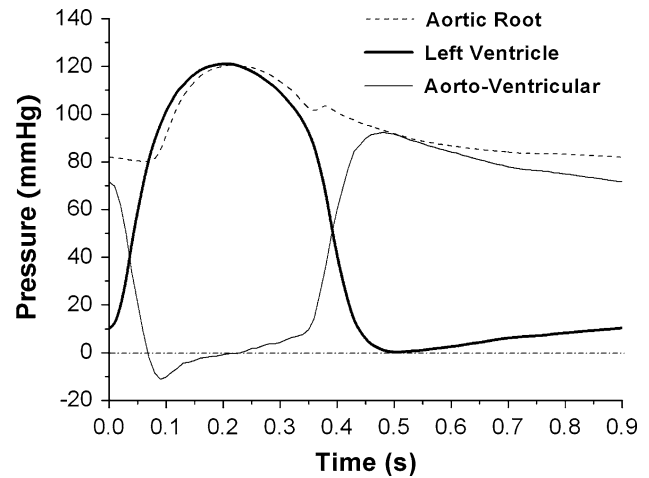
FIGURE 2. Time-varying pressure loadings over a full cardiac cycle.

In Vitro Validation

Two physical models with identical geometry and size to the SPAC tubular valve and the SPAC molded valve in the finite element study were tested in a pulsatile mock-circulatory system (ViVitro Systems Inc., Victoria, BC, Canada). A typical test model consists of a silicone aortic root and valve leaflets made from porcine pericardium. Pressure waveforms in the left ventricle, the left atrium, and the aorta were monitored and recorded. The compliance and resistance units were adjusted to make sure that the pulsatility index and the shape of the pressure waveforms conform to those in the finite element study. A borescope was inserted at the top of the aortic root assembly to record the opening and closing of the valve leaflets.

RESULTS

Dynamic Behavior

Finite Element Results

The generic features in dynamic behavior for all the three models investigated include large deformation and extremely rapid motion of the valve leaflets during the opening and closing and the dynamic rocking motion of the aortic root throughout the cardiac cycle. Selected frames of the displacements for each model during a full cardiac cycle of 0.9 s are displayed in Fig. 3, in which the times are counted from $t = 0$ s of the dynamic pressure waveforms (Fig. 2) when the valve leaflets have been displaced to the closed diastolic configuration. Detailed dynamic behavior of the SPAC molded and the SPAC tubular valve models can be viewed in the supplemental movie files (Videos 1 and 2).

For all the three models, the valve begins to open when the aortic pressure is still higher than the left ventricular pressure. The opening begins at $t = 0.036$, 0.048, and 0.047 s for the tubular valve, the molded valve, and the conventional valve, respectively. During the intermediate period of the valve opening, the partially opened valve first produces a stellate-shaped orifice (Fig. 3, $t = 0.064$ s), which then changes into a clover shape with the central part of the free edges concaved toward the center of the valve (Fig. 3, $t = 0.068$ s). At $t = 0.070$ s when the left ventricular pressure just exceeds the aortic pressure, all three valves have already reached the fully opened position. The time required for opening the valve is about 0.034, 0.022, and 0.023 s for the tubular valve, the molded valve, and the conventional valve, respectively.

The fully opened tubular valve exhibits a triangular orifice (Fig. 3, $t = 0.170$ s); the maximum EVOA is 400.6 mm^2, the leaflet surface area is 575.0 mm^2, and the free edge length is 28.3 mm. In contrast, for the molded valve and the conventional valve reaching the fully opened position, the free edges move further apart forming a circular orifice (Fig. 3, $t = 0.170$ s). The maximum EVOA, the leaflet surface area, and the free edge length for the molded valve are 633.5 mm^2, 633.1 mm^2, and 29.4 mm, respectively. The corresponding values for the conventional valve are 630.8 mm^2, 571.5 mm^2, and 29.3 mm. The maximum radial expansion of the commissures is reached at peak systole ($t = 0.210$ s), being 1.84, 2.61, and 2.81 mm from the initial stress-free position for the tubular valve, the molded valve, and the conventional valve, respectively, corresponding to an expansibility of 7.4%, 10.4%, and 11.2% in relation to the aortic root diameter.

The fully opened phase lasts until $t = 0.275$, 0.300, and 0.278 s for the tubular valve, the molded valve, and the conventional valve, respectively, when valve closure starts. For all three models, as the leaflets continue to move toward the valve center, the orifice again exhibits a stellate shape, similar to that observed during valve opening (Fig. 3, $t = 0.300$–0.350 s). It is not until $t = 0.395$ s has the tubular valve become completely closed. In contrast, the closing of the molded valve and the conventional valve begins later, but complete closure arrives at $t = 0.377$ s, which is earlier than the tubular valve.

For the molded valve and the conventional valve, as the leaflets coaptate against each other, the free-edges form S-shaped lines, with the central parts twisting counterclockwise, and the inertial effect of the dynamic motion during valve closure tends to twist further the free edges (Fig. 3, $t = 0.560$ s). In contrast, the free-edge lines in the closed tubular valve are fairly straight (Fig. 3, $t = 0.560$ s). The leaflet surface area and the free-edge length for the fully closed tubular valve are 574.3 mm^2 and 29.4 mm, respectively. The corresponding values are 629.7 mm^2 and 30.0 mm for the molded valve, and 569.0 mm^2 and 29.9 mm for the conventional valve.
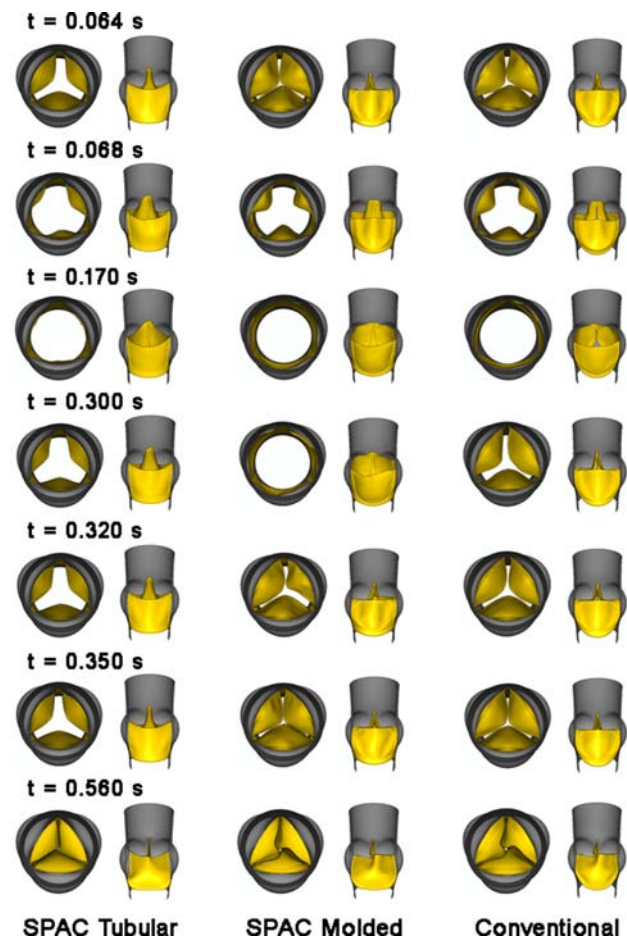

FIGURE 3. Selected frames of dynamic displacements during the full cardiac cycle for the SPAC tubular, SPAC molded, and conventional valve models. Both a top view and a lateral view are shown for each model at each moment.

In Vitro Results

The *in vitro* results included only the dynamic behavior of the SPAC molded and the tubular valve models, which are shown in the supplemental movie files (Videos 3 and 4). Measurement of other parameters such as leaflet opening and closing times, leaflet stress, and coaptation area for validation are difficult to perform with the current experimental settings. The *in vitro* results also demonstrate a large deformation and rapid motion of the valve leaflets during opening and closing and the drastic radial motion of the aortic root. Distinct differences between the two valves can

be observed, particularly in the fully opened and the fully closed positions. The molded valve, when fully opened, produces a greater EVOA than the tubular valve, and when fully closed, is sealed more completely and firmly. The images captured in the fully closed position (Fig. 4) show that the free edges in the molded valve form curved lines, whereas the free-edge lines in the tubular valve are straight. It can also be observed that the movement of the leaflets of the molded valve is smooth, in contrast to the stiff movement of those of the tubular valve.

Coaptation Parameters

The maximum coaptation height in the molded valve and the conventional valve is 4.4–4.5 mm vs. 1.2 mm in the tubular valve (Fig. 5). It appears that in the tubular valve, only the margins of the free edges participate in coaptation. The area for coaptation varying over the cardiac cycle for a single leaflet is plotted in Fig. 6 for all the three models. The coaptation area during valve closing is generally greater in the molded valve and the conventional valve than in the tubular valve. The maximum coaptation area in the tubular valve, the molded valve, and the conventional valve is 238.5, 386.1, and 294.1 mm^2, respectively.

Leaflet Stress Distributions

Figures 7 and 8 show, respectively, the distributions of compressive stress and Von Mises stress for all three models at the fully closed position when the maximum stress magnitudes are found. Compressive stress occurs on the aortic surface of the leaflet. For the tubular valve, the highest magnitude in compressive stress is found at the commissures, and the second highest along the inter-leaflet margin and the leaflet basal attachment line. For the molded valve and the conventional valve, the localization of
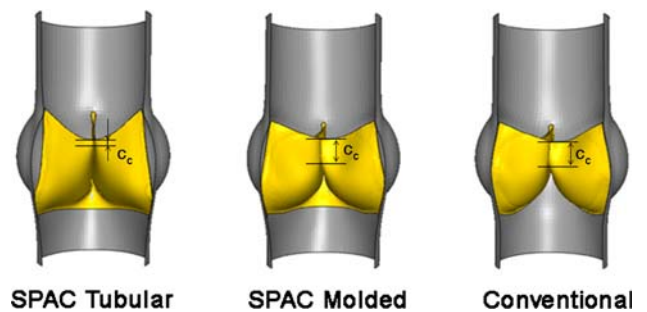

FIGURE 5. Coaptation height of the SPAC tubular, SPAC molded, and conventional valve models. One-third of the aortic root and the valve is removed for visualization.
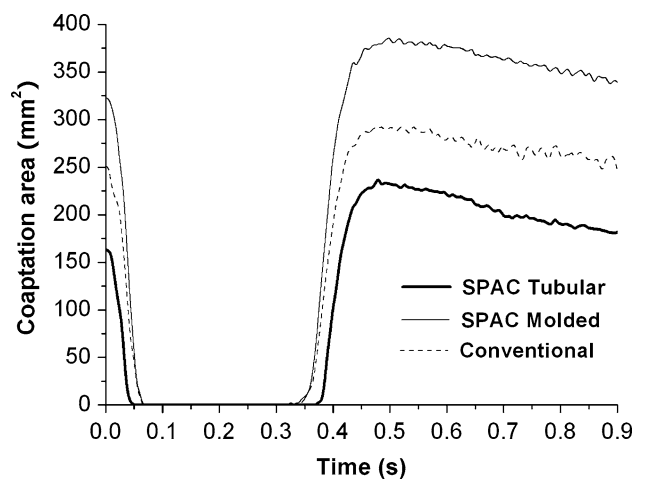

FIGURE 6. Comparison of area participating in coaptation for a single leaflet varying over the cardiac cycle, between the SPAC tubular, SPAC molded, and conventional valve models.

compressive stress is different, the highest magnitude being near the center of the free edge and the second highest on the leaflet belly, showing only moderately elevated values. The highest magnitude in the tubular valve is more than twice that in the molded valve (Table 1).

Similarities exist in the distribution patterns of Von Mises stress for all the three valves, showing the highest level at the commissures and the second highest at the leaflet basal attachment region and along the inter-leaflet margin. A dynamic impact during valve closure causes a sudden increase in stress, particularly at the commissures and the valve center. The highest stress at the commissures in the molded valve is slightly higher than that in the tubular valve, and slightly lower than that in the conventional valve (Table 1). Regions of relatively high stress also include the leaflet belly of the tubular valve and the central part of the free edge of all the three valves.

FIGURE 4. Images of the SPAC tubular valve and the SPAC molded valve in the fully closed position captured from the *in vitro* video results.
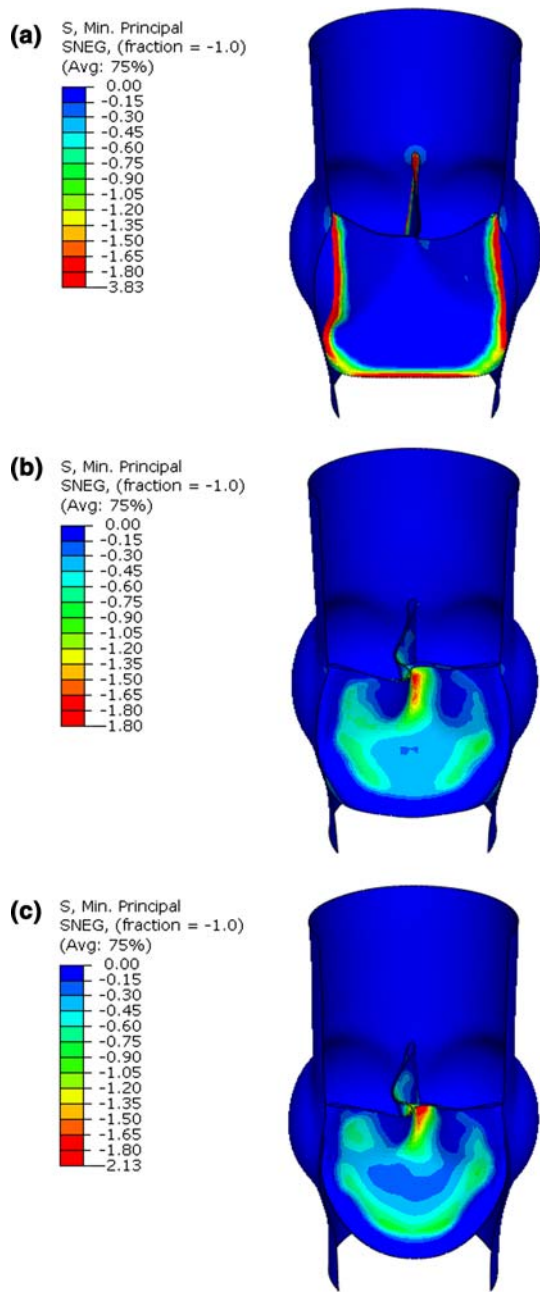
FIGURE 7. Distributions of compressive stress (MPa) for (a) SPAC tubular, (b) SPAC molded, and (c) conventional valve models. One-third of the aortic root is removed for visualization of the internal structure.
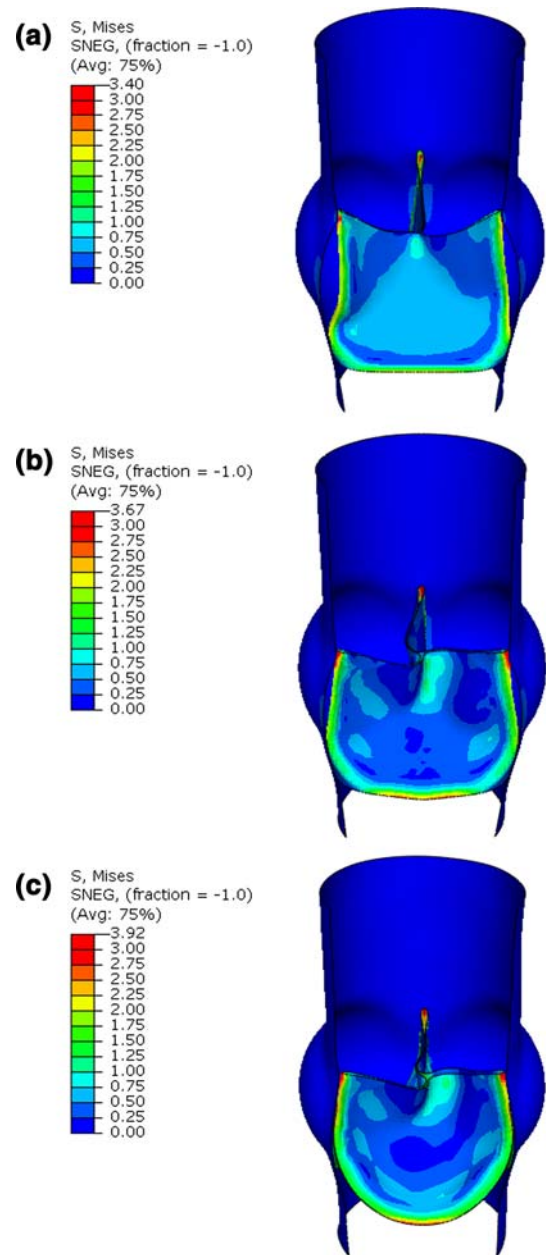
FIGURE 8. Distributions of Von Mises stress (MPa) for (a) SPAC tubular, (b) SPAC molded, and (c) conventional valve models. One-third of the aortic root is removed for visualization of the internal structure.

DISCUSSION

Clinical experiences of the SPAC tubular valve show that the SPAC approach indeed facilitates implantation, but the valve performance is only comparable to regular stentless aortic valves despite its advantages of containing less obstructive material and being simpler and faster in implantation.[12,16] We speculate that the simple tubular leaflet geometry may be a major compromising factor on the outcome. The SPAC molded valve has recently emerged as a possible alternative to the tubular design, and this valve is featured by a complex 3D leaflet geometry defined using specially designed valve molds. The method of fabricating a SPAC molded valve using valve molds and pericardial tissue can be found in the literature.[15] This study tests the hypothesis that the molded 3D leaflet geometry

which resembles the native aortic valve would improve mechanical performance of the SPAC pericardial valves compared to the simple tubular leaflet design.

In the present study, the full structure of the valve incorporating the compliant aortic root and sinuses was modeled. The drastic motion of the aortic root during the cardiac cycle is demonstrated. One important role of the movement of the aortic root wall, as has been suggested, is to aid in the opening and closing of the leaflets.[31] As the aortic root wall moves, it carries the leaflets along with it, particularly at the commissures. The commissures move outward during systole and inward during diastole closely following the curve of the aortic pressure. The maximum radial expansibility of the commissures is found to be 10.4–11.2% in the SPAC molded valve and the conventional valve models, within the physiological range.[4] Also noted is that for all the models investigated, the leaflets begin to open and produce a stellate orifice even before the left ventricular pressure exceeds the aortic pressure, which results primarily from the outward movement of the sinotubular junction that starts before the valve opening, a typical phenomenon seen in native aortic valves.[31] The dynamic interplay between the compliant aortic root and the valve leaflets as an integrated system has been recognized to be important in the optimal functioning of the aortic valve,[13,30] even unintentionally present in our current numerical and *in vitro* models.

The characteristics of a functioning aortic valve include the rapid motion of the leaflets during opening and closing, the nonobstructive maximized orifice of the open valve, as well as the firmly sealed leaflets of the closed valve. This study shows that while all valves investigated are able to provide normal functioning, there are distinct differences which result from the difference in leaflet geometry between the SPAC molded valve and the SPAC tubular valve. First, significantly less time is required for opening and closing the molded valve than the tubular valve. The opening process takes about 0.022 s for the former vs. 0.034 s for the latter. This observation suggests that the leaflet mobility may be better with the molded leaflet design. Second, leaflet geometric configuration clearly affects the characteristics of the open valve during systole. The maximum radial expansibility of the commissures for the molded valve is found to be 10.4% vs. 7.4% in the tubular valve. Along with a reduced commissural expansibility in the tubular valve, the EVOA is substantially reduced. The molded valve exhibits a wide nearly circular orifice, whereas the orifice of the tubular valve is narrower and triangular-shaped. The free-edge length is the primary geometric factor causing these differences since after systolic radial extension of the commissures, a shorter free edge becomes effective and restricts the further outward movement of the leaflets. Third, as the leaflets seal against each other at the fully closed position, the free edges in the molded leaflet design form S-shaped lines, characterized by twisting at the valve center, while the tubular design shows straight free-edge lines. This observation again can be explained by the difference in leaflet geometry and free-edge length: the more anatomically correct geometry and longer free-edge length in the molded valve ensure a better coaptation of the leaflets and provide more safety for closure. Indeed, further examination of the coaptation parameters reveals that the coaptation height, a critical parameter for assessing valve competence, is measured to be 4.5 mm in the molded valve, nearly four times greater than in the tubular valve, suggesting the former may be more competent. To verify the numerical results, the validation study shows that the typical behavior of the molded and the tubular valves predicted by the numerical study agrees reasonably with the *in vitro* results. For example, the distinct differences in EVOA and shape of coaptation lines between the molded valve and the tubular valve are demonstrated by both the numerical and the *in vitro* studies.

Calcification and structural deterioration are the main causes of failure of bioprosthetic aortic valves. There is evidence that calcification is initiated and/or accelerated by tissue degeneration caused by mechanical stresses.[11,32] Thubrikar *et al.* demonstrated *in vivo* a close correlation between areas of high compressive stress and calcification in porcine bioprosthetic valves, and suggested that compressive stress may cause calcification by inducing fiber separation and opening of cavities of the local tissue.[32] Our results show significant differences in both localization and magnitude of compressive stress between the tubular valve and the molded valve. For the tubular valve, high compressive stress prevails at the commissures, and along the interleaflet margin and the leaflet basal attachment line. For the molded valve, compressive stress is completely absent in the corresponding regions; instead, it is found near the center of the free edge and on the leaflet belly. The highest stress magnitude in the tubular valve is more than twice that in the molded valve. As compressive stress plays an important role in the pathogenesis of early structural valve deterioration,[32] this study suggests that calcification in the tubular valve would be markedly more severe than in the molded valve, and would develop in different regions. The observation of the highest compressive stress being at the center of the free edge of the molded valve suggests the possible role of the nodule of Arantius in native aortic valves for sustaining high stress, and emphasizes the importance of reproducing or mimicking such a

functional component in designing bioprosthetic aortic valves, if technically feasible.

In addition to compressive stress, the bioprosthetic leaflets may also fail from tensile stress and shear stress. For example, high shear stress is likely to disrupt the structural integrity of pericardial leaflet tissue along the planes of shear by the sliding of individual layers of collagen over each other, forming sites for calcification.[32] The Von Mises stress accounts for multiple effects of all stress components on a material. Our results show that all valves exhibit the highest level of Von Mises stress at the commissures and the second highest at the basal attachment region and along the inter-leaflet margin. These are regions that may be predisposed to calcification and structural failure. The highest stress at the commissures in the SPAC molded valve is found to be slightly higher than in the SPAC tubular valve by 6.5%. In contrast to this observation are results from Lim et al., who compared a 3D leaflet geometry similar to that in our study with a flat leaflet geometry using a static finite element analysis.[23] They reported a 34.5% reduction in Von Mises stress at the commissures in the 3D leaflet model and suggested the improved leaflet geometry and longer free edge to be the main cause for the reduction. The discrepancy between their study and the present one is presumably due to the differences in the nature of analysis (static vs. dynamic) and the boundary conditions used. They simulated only one-sixth of the valve with symmetry assumed and specified the symmetry plane to be a fictitious coaptation plane where the leaflets should meet. In the present study, with a full valve being simulated and more realistic boundary conditions assigned, we found that the molded valve, when the leaflets coaptate, becomes an asymmetric structure due to the counterclockwise twisting of the free edges at the valve center. A dynamic impact during valve closure twists further the free edges, causing a sudden and simultaneous increase in stress at the commissures and the valve center. Such a twisting effect, when it is severe, tends to increase the strain of the free edge and hence higher stress at the commissural attachment points, which may explain our results that the maximum Von Mises stress at the commissures is higher in the molded valve than in the tubular valve.

The SPAC implantation approach, with proven efficacy by *in vitro* and *in vivo* studies as well as human implants,[8,12,14–16,25] has been gaining increasing attention. Still of interest is its exact influence on valve functioning and mechanics. Comparison of the SPAC molded valve and the conventional valve in our study shows that the SPAC approach slightly affects the outward expansion of the commissures during systole. The maximum commissural expansibility is 10.4% in the molded valve, vs. 11.2% in the conventional valve.

Another interesting finding is that the SPAC approach tends to reduce the maximum magnitude in both compressive stress and Von Mises stress. These differences should result primarily from the change in distribution of loadings caused by the difference in implantation approach: for the conventional approach the leaflets are attached to the aortic root along the scalloped native leaflet attachment line with the inter-leaflet triangles subjected to the left ventricular pressure, whereas for the SPAC approach the leaflets are attached at the commissural points and along a circular base with the inter-leaflet triangles subjected to the aortic pressure. Despite the differences, our results indicate that the SPAC approach does not compromise the overall valve performance in comparison to the conventional approach, as it does not appreciably alter the timings of the leaflet opening and closure, EVOA, coaptation height, as well as the overall stress distribution patterns.

The results from the present study may also have implications for the design of tissue-engineered heart valve scaffolds. Biologically derived soft tissues for manufacturing bioprostheses including the pericardial tissue used in SPAC valves usually need to be cross-linked with glutaraldehyde before implantation to reduce their antigenicity and to stabilize the tissue against the proteolytic degradation. This process predisposes the tissue to calcification and greatly reduces its durability. Tissue-engineered heart valves, which consists of autologous and viable tissue, have been proposed to eliminate the problems of the existing bioprosthetic valves. One way to construct a tissue-engineered heart valve is to utilize a synthetic biodegradable porous scaffold seeded with living cells, which, when implanted in the body, can generate the organ of interest such as the aortic valve as the scaffold degenerates. It has recently been found that certain synthetic biodegradable materials can be fabricated to resemble the mechanical and structural properties and even the fiber network of the native valve tissue.[7] A synthetic tissue-engineered heart valve scaffold, like the pericardial bioprosthetic valves, is amenable for major variations in its leaflet geometric design. However, the leaflet geometry of the scaffold has not been a major concern for current heart valve scaffold designers.[7,29] The present study has demonstrated that a leaflet geometry that resembles the native aortic valve has a favorable influence on the dynamic behavior of the SPAC pericardial valves. We believe that the performance of the tissue-engineered heart valves can also be improved by designing the leaflet geometry of the scaffolds to resemble the native valves. Valve molds may be useful in the fabrication of scaffolds with such a complex leaflet geometry.

It is essential to properly validate the finite element model against experiments to verify the accuracy of the numerically predicted results. We have performed a simple qualitative validation using videos recorded from the Vivitro pulse duplicator system. A more rigorous and quantitative validation is challenging for our *in vitro* study, as we found it difficult to quantify even the basic valve performance parameters such as leaflet deformation and displacement. In fact, for most finite element studies of bioprosthetic aortic valves, due to the difficulty of quantitative experimental measurement, validation has either not been performed[2,13,22,30] or has been performed qualitatively by comparing transient leaflet deformations using images from a pulse duplicator system.[5,19] Recently, Haj-Ali *et al.* presented a validation method that offers quantitative comparisons between experimentally measured and numerically predicted leaflet behaviors.[17] This method, however, may not be applicable to our study because of the different materials used for fabricating the valve leaflets. The silicone-based polyurethane copolymers they used for their *in vitro* valve model is more rigid and therefore should make it easier to quantify leaflet deformation and displacement than the soft porcine pericardial tissue used for the models in our *in vitro* study. Although our validation is simple, it can show, at least, that some typical results predicted by the finite element study such as the differences in EVOA and shape of coaptation lines between the tubular and the molded valves are meaningful.

We simulated only the solid part while neglecting the fluid part by substituting time-varying spatially uniform pressure loadings for fluid forces, which is admittedly a major limitation of the present study. Aortic valve dynamics is characterized by strong interactions between flow dynamics and the motions of the aortic root wall and the valve leaflets. For example, the rapid closure of the valve during diastole is largely associated with the flow vorticity dynamics beneath the leaflets.[9] Variations of local flow dynamics in different regions also result in complex regional variations of pressure, particularly in the vicinity of the leaflets and sinus of Valsalva. We admit that incorporating fluid–structure interaction (FSI) will afford a more realistic representation of aortic valve dynamics. However, for the specific problem investigated in the present study, modeling of FSI is computationally difficult, if not impossible. As demonstrated in our *in vitro* study, the asymmetric coaptation of the leaflets and twisting of the free edges are typical of the molded valve. Modeling this typical behavior of the molded valve requires using the full 3D model and simulating the complex highly nonlinear contact between the leaflets, which would both greatly increase the computational difficulty. These issues are important and have not yet been

resolved with the existing FSI models. Take for instance the work of de Hart *et al.*[10] Two major simplifications are noteworthy in their FSI model. First, they simulated only one-sixth of the valve model (i.e., one-half of a leaflet and sinus of Valsalva) by assuming axisymmetry in model geometry. Second, they forcibly bound the leaflet in circumferential direction by two symmetry surfaces, presumably to avoid the difficulty of modeling contact between the adjacent leaflets. Although their model successfully simulated FSI, it would not be capable of describing the natural contact behavior and the asymmetric coaptation between the leaflets. We therefore chose to use the solid-only models to address these issues. Although our solid-only models may not accurately predict every detail of the behavior of the valves, comparisons with the *in vitro* results showed that at least some typical characteristics are reasonably well captured. The study of Carmody *et al.* may lend more support to the use of solid-only models for modeling aortic valves.[6] By simulating FSI of the aortic valve, they found that the pressure difference across the leaflets is essentially uniform and they further concluded that it is reasonable to use spatially uniform but temporally variable pressure distributions across the leaflets in dry or structural models of aortic valves.[6]

We used homogeneous and isotropic materials for all the finite element models, out of concern of the numerical difficulty. The finite element model used in this study involves the coupling of the motions of the valve and the aortic root, the large displacement and flexion of the valve leaflets, as well as the nonlinear dynamic contact between the three leaflets and between the leaflets and the aortic root, which greatly complicated the analysis, causing difficulty for convergence. Incorporating material anisotropy and nonlinearity would further add to the convergence difficulty. It has been found that a linear assumption of the leaflet material exerts certain effects on leaflet stress and deformation.[22,27] However, our main goal was to study the effect of the different leaflet geometries, which is still possible with the linear assumption as any potential bias for each model resulting from this assumption would always point in the same direction. Thus, the use of material nonlinearity would not essentially change the conclusions reached in this study. Anisotropy has been demonstrated in fresh collagenous soft tissues, but it is not definitive for chemically treated pericardial tissue. The inconsistent results may be due to the fixation method being variable among different studies. Nevertheless, we recognize the importance of both retaining and modeling anisotropy and nonlinearity for biologically derived tissue aortic valves. For example, a great number of studies suggest that retaining anisotropy for tissue

aortic valves during the bioprosthesis manufacturing process to mimic the native one may optimize the valve dynamic response and reduce the leaflet stress during function, which may provide a greater resistance to fatigue.[2,3,20,22,24] The simplified constitutive model in the present study may act as a base to be gradually refined toward a more descriptive and accurate one in our future studies.

CONCLUSIONS

The molded 3D leaflet geometry resembling the native valve exerts a positive influence on the mechanical performance of the SPAC pericardial aortic valves compared with the simple tubular leaflet geometry, as it contributes to better dynamic leaflet behavior, increased EVOA, increased leaflet coaptation height and area, and reduced compressive stress. We believe that leaflet geometry is relevant to the efficacy and durability of the SPAC pericardial aortic valves and can be optimized through numerical studies. Additionally, the SPAC implantation approach does not seem to compromise the valve mechanical performance for all the parameters examined here, as compared with the conventional approach.

ELECTRONIC SUPPLEMENTARY MATERIAL

ACKNOWLEDGMENT

REFERENCES

[1]Akar, A. R., A. Szafranek, C. Alexious, R. Janas, M. J. Jasinski, J. Swanevelder, and A. W. Sosnowski. Use of stentless xenografts in the aortic position: determinants of early and late outcome. *Ann. Thorac. Surg.* 74:1450–1457, 2002.

[2]Arcidiacono, G., A. Corvi, and T. Severi. Functional analysis of bioprosthetic heart valves. *J. Biomech.* 38:1483–1490, 2005.

[3]Billiar, K. L., and M. S. Sacks. Biaxial mechanical properties of the native and glutaraldehyde-treated aortic valve cusp: Part I. Experimental results. *ASME J. Biomech. Eng.* 122:23–30, 2000.

[4]Brewer, R. J., J. D. Deck, B. Capati, and S. P. Nolan. The dynamic aortic root—its role in aortic valve function. *J. Thorac. Cardiovasc. Surg.* 72:413–417, 1976.

[5]Cacciola, G., G. W. M. Peters, and P. J. G. Schreurs. A three-dimensional mechanical analysis of a stentless fibre-reinforced aortic valve prosthesis. *J. Biomech.* 33:521–530, 2000.

[6]Carmody, C. J., G. Burriesci, I. C. Howard, and E. A. Patterson. An approach to the simulation of fluid–structure interaction in the aortic valve. *J. Biomech.* 39:158–169, 2006.

[7]Courtney, T., M. S. Sacks, J. Stankus, J. Guan, and W. R. Wagner. Design and analysis of tissue engineering scaffolds that mimic soft tissue mechanical anisotropy. *Biomaterials* 27(19):3631–3638, 2006.

[8]Cox, J. L., N. Ad, K. Myers, M. Gharib, and R. C. Quijano. Tubular heart valves: a new tissue prosthesis design—preclinical evaluation of the 3F aortic bioprosthesis. *J. Thorac. Cardiovasc. Surg.* 130(2):520–527, 2005.

[9]Dasi, L. P., H. A. Simon, P. Sucosky, and A. P. Yoganathan. Fluid mechanics of artificial heart valves. *Clin. Exp. Pharmacol. Physiol.* 36(2):225–237, 2009.

[10]De Hart, J., G. W. M. Peters, P. J. G. Schreurs, and F. P. T. Baaijens. A three-dimensional computational analysis of fluid-structure interaction in the aortic valve. *J. Biomech.* 36:103–112, 2003.

[11]Deiwick, M., B. Glasmacher, H. A. Baba, N. Roeder, H. Reul, G. von Bally, and H. H. Scheld. In vitro testing of bioprostheses: influence of mechanical stresses and lipids on calcification. *Ann. Thorac. Surg.* 66(6 Suppl):S206–S211, 1998.

[12]Doss, M., S. Martens, J. P. Wood, A. Miskovic, T. Christodoulou, G. Wimmer-Greinecker, and A. Moritz. Aortic leaflet replacement with the new 3F stentless aortic bioprosthesis. *Ann. Thorac. Surg.* 79(2):682–685, 2005.

[13]Gnyaneshwar, R., R. K. Kumar, and K. R. Balakrishnan. Dynamic analysis of the aortic valve using a finite element model. *Ann. Thorac. Surg.* 73:1122–1129, 2002.

[14]Goetz, W. A., K. H. Lim, R. Ibled, N. Grousson, S. Salgues, and J. H. Yeo. Forces at single point attached commissures (SPAC) in pericardial aortic valve prosthesis. *Eur. J. Cardiothorac. Surg.* 29:150–155, 2006.

[15]Goetz, W. A., T. E. Tan, K. H. Lim, S. Salgues, N. Grousson, F. Xiong, Y. L. Chua, and J. H. Yeo. Truly stentless molded autologous pericardial aortic valve prosthesis with single point attached commissures in a sheep model. *Eur. J. Cardiothorac. Surg.* 33:548–553, 2008.

[16]Grubitzsch, H., J. Linneweber, C. Kossagk, E. Sanli, S. Beholz, and W. Konertz. Aortic valve replacement with new-generation stentless pericardial valves: short-term clinical and hemodynamic results. *J. Heart Valve Dis.* 14(5):623–629, 2005.

[17]Haj-Ali, R., L. P. Dasi, H. Kim, J. Choi, H. W. Leo, and A. P. Yoganathan. Structural simulations of prosthetic tri-leaflet aortic heart valves. *J. Biomech.* 41:1510–1519, 2008.

[18]Hanlon, J. G., R. W. Suggit, and J. W. Love. Preuse intraoperative testing of autologous tissue for valvular surgery: a proof of concept study. *J. Heart Valve Dis.* 8:614–624, 1999.

[19]Kim, H., K. B. Chandran, M. S. Sacks, and J. Lu. An experimentally derived stress resultant shell model for heart

valve dynamic simulations. *Ann. Biomed. Eng.* 35(1):30–44, 2007.

[20] Kim, H., J. Lu, M. S. Sacks, and K. B. Chandran. Dynamic simulation of bioprosthetic heart valves using a stress resultant shell model. *Ann. Biomed. Eng.* 36(2):262–275, 2008.

[21] Lee, J. M., S. A. Haberer, and D. R. Boughner. The bovine pericardial xenograft: I. Effect of fixation in aldehydes without constraint on the tensile viscoelastic properties of bovine pericardium. *J. Biomed. Mater. Res.* 23:457–475, 1989.

[22] Li, J., X. Y. Luo, and Z. B. Kuang. A nonlinear anisotropic model for porcine aortic heart valves. *J. Biomech.* 34:1279–1289, 2001.

[23] Lim, K. H., J. Candra, J. H. Yeo, and C. M. Duran. Flat or curved pericardial aortic valve cusps: a finite element study. *J. Heart Valve Dis.* 13(5):792–797, 2004.

[24] Mirnajafi, A., J. Raymer, M. J. Scott, and M. S. Sacks. The effects of collagen fiber orientation on the flexural properties of pericardial heterograft biomaterials. *Biomaterials* 26:795–804, 2005.

[25] Mueller, X., and L. K. von Segesser. A new equine pericardial stentless valve. *J. Thorac. Cardiovasc. Surg.* 125(6):1405–1411, 2003.

[26] O'Brien valve, M. F. The Cryolife-O'Brien composite aortic stentless xenograft: surgical technique of implantation. *Ann. Thorac. Surg.* 60(2 Suppl):S410–S413, 1995.

[27] Patterson, E. A., I. C. Howard, and M. A. Thornton. A comparative study of linear and nonlinear simulations of the leaflets in a bioprosthetic heart valve during the cardiac cycle. *J. Med. Eng. Technol.* 20:95–108, 1996.

[28] Rao, V., G. T. Christakis, J. Sever, S. E. Fremes, G. Bhatnagar, G. Cohen, M. A. Borger, L. Abouzahr, B. S. Goldman, and C. F. Sintek. A novel comparison of stentless versus stented valves in the small aortic root. *J. Thorac. Cardiovasc. Surg.* 117:431–438, 1999.

[29] Sodian, R., S. P. Hoerstrup, J. S. Sperling, S. H. Daebritz, D. P. Martin, F. J. Schoen, J. P. Vacanti, and J. E. Mayer. Tissue engineering of heart valves: in vitro experiences. *Ann. Thorac. Surg.* 70:140–144, 2000.

[30] Sripathi, V. C., R. K. Kumar, and K. R. Balakrishnan. Further insights into normal aortic valve function: role of a compliant aortic root on leaflet opening and valve orifice area. *Ann. Thorac. Surg.* 77:844–851, 2004.

[31] Thubrikar, M. J. The Aortic Valve. Boca Raton, FL: CRC Press, 1990.

[32] Thubrikar, M. J., J. D. Deck, J. Aouad, and S. P. Nolan. Role of mechanical stress in calcification of aortic bioprosthetic valves. *J. Thorac. Cardiovasc. Surg.* 86(1):115–125, 1983.

[33] Yoganathan, A. P., and B. R. Travis. Fluid dynamics of prosthetic valves. In: The Practice of Clinical Echocardiography, edited by C. M. Otto. Philedelphia, PA: WB Saunders, 2000.

[34] Zioupos, P., J. C. Barbenel, and J. Fisher. Anisotropic elasticity and strength of glutaraldehyde fixed bovine pericardium for use in pericardial bioprosthetic valves. *J. Biomed. Mater. Res.* 28:49–57, 1994.